Bronchiolitis Obliterans and Pneumonia Induced in Young Dogs by Experimental Adenovirus Infection

WILLIAM L. CASTLEMAN, DVM, PhD

From the Department of Pathology, New York State College of Veterinary Medicine, Cornell University, Ithaca, New York

Young beagle dogs were experimentally inoculated with canine adenovirus Type 2 and studied by virologic, histologic, immunoperoxidase, and ultrastructural methods from 1 to 26 days after inoculation. Virus was recovered from lungs at 2, 3, 5, and 8 days after inoculation. Virions and viral antigen were demonstrated by ultrastructural and immunoperoxidase techniques in nonciliated bronchiolar epithelial cells and mucous cells in bronchioles, bronchi, and trachea as well as in bronchial and tracheal submucosal gland epithelial cells. Viral replication in airways was associated with a severe necrotizing and proliferative bronchitis and bronchiolitis. Virus and viral antigen were demonstrated in Type 2 alveolar epithelial cells and were associated with interstitial pneumonia. Partial and complete stenosis of bronchioles by connective tissue was observed at 15 and 26 days after inoculation. There was a 50% reduction ($P < 0.02$) in mean terminal bronchiolar cross-sectional area in the right middle lobe of virus-infected dogs at 26 days after inoculation. It is concluded that experimental adenovirus infection in dogs induces bronchiolitis obliterans and that this experimental model may be useful for studies on adenovirus-induced lung injury during early life. (Am J Pathol 1985, 119:495–504)

VIRAL RESPIRATORY infection in early life is a common event resulting in acute clinical disease as well as chronic sequelae.[1-3] Physiologic and epidemiologic studies indicate that viral infection during the first 2 years of infancy may result in persistent abnormalities in lung function such as increased airway resistance,[1-7] and that this early episode of viral respiratory disease may predispose individuals to chronic respiratory disease in later life.[8-10]

Adenovirus infection has been reported to be associated with between 2% and 13% of the cases of bronchiolitis in children less than 2 years of age[5,10] and in some instances has been associated with especially severe respiratory disease.[4,11-16] Pathologic changes reported in fatal cases of adenoviral respiratory disease in children have included severe necrotizing bronchitis with necrosis of bronchial glandular epithelium, bronchiectasis, necrotizing bronchiolitis, and bronchiolitis obliterans as well as pneumonia and pulmonary fibrosis.[4,11-16]

Experimental models for the study of virologic, immunologic, and structural events during viral respiratory disease in early life have been developed.[17-24] Most of these focus on the effects of respiratory syncytial virus or parainfluenza.[17-21] Experimental models of adenoviral bronchiolitis that would be useful for studies on identification of important pathogenetic mechanisms as well as on therapeutic modulation of injury are limited in number and have not been characterized in detail.[22-24]

This report characterizes an experimental model of adenoviral infection during early life that uses a natural adenoviral respiratory pathogen of dogs. The morphogenesis and repair of bronchiolitis and pneumonia in relation to viral replication as well as the development of bronchiolitis obliterans are described using this model.

Materials and Methods

Dogs and Virus

Twenty specific-pathogen-free (SPF), 12-week-old beagle dogs were used in the study. They were obtained at 11 weeks of age from the SPF dog breeding colony, Division of Laboratory Animal Services, Cornell University, and housed in isolation rooms for 1 week before being infected. The dogs were randomly assigned to infected and control groups. The dogs were assessed

Accepted for publication February 1, 1985.

Address reprint requests to Dr. William L. Castleman, Department of Pathology, N.Y.S. College of Veterinary Medicine, Cornell University, Ithaca, NY 14853.

to be normal by clinical evaluation and were free of *Bordetella bronchiseptica*, parainfluenza virus, canine distemper virus, and canine parvovirus as determined by routine microbiologic and viral serologic methods. The dogs had low antibody titers to canine adenovirus derived from the vaccinated bitches. Fifteen dogs were inoculated by the intratracheal route with 1×10^6 50% tissue culture infective doses ($TCID_{50}$) of canine adenovirus Type 2 (CAV-2) diluted in phosphate-buffered saline solution (PBSS) to a total volume of 6 ml. The dogs were tranquilized with acepromazine (0.55 mg/kg) before intramuscular inoculation. The virus was injected intraluminally at the midcervical region of the trachea after placement of a 20-gauge syringe needle through the skin and tracheal wall. The Manhattan strain of the virus[25] was generously supplied by Dr. Max Appel at Cornell University and was produced by replication in Madin–Darby canine kidney (MDCK) cells. Five dogs were sham-inoculated with 6 ml of PBSS intratracheally and served as controls. The dogs were observed daily for clinical signs of disease and underwent necropsy after anesthesia with sodium pentobarbital and death induced by exsanguination and pneumothorax. Infected dogs underwent necropsy on the following days after inoculation: 1 dog each at Days 1 and 2 after inoculation; 2 dogs each at days 3, 4, 5, 8, and 15; and 3 dogs at 26 days after inoculation. Two control dogs underwent necropsy at 3 days, and 3 were studied at 26 days after sham inoculation.

Histology and Electron Microscopy

The right lung was fixed via the trachea at 30 cm pressure with modified Karnovsky's fixative and processed for light microscopy and scanning and transmission electron microscopy as previously described.[21,26] Nine sections were taken from each dog from the right cranial, middle, and caudal lung lobes in a uniform manner for paraffin embedding so that dorsal, ventral, and hilar samples of tissue could be studied histologically. At least four blocks of tissue were taken from peripheral ventral and dorsal areas of lung in addition to trachea and were embedded in Epon–Araldite for preparation of plastic sections with a Sorvall JB-4 microtome. Small blocks from areas of interest were dissected from the JB-4 blocks and mounted on plastic blocks so that they could be sectioned for electron microscopy. A total of at least 6 ultrathin sections from each dog that included trachea, bronchus, terminal or respiratory bronchiole, and alveolar parenchyma were stained with uranyl acetate and lead citrate and were examined with a transmission electron microscope. Selected sections of terminal bronchiole and alveolar parenchyma from infected and control dogs at 3 and 26 days after inoculation were prepared for scanning electron microscopy as described[26] for characterization of alterations in ciliated mucosal epithelium.

Morphometrics

Volumes of the right lungs at 26 days after inoculation were determined by fluid displacement.[27] Terminal bronchiolar cross-sectional areas were determined as previously described.[21] Briefly, transverse sections of terminal bronchioles from the paraffin sections stained with hematoxylin and eosin (H&E) were photographed. Terminal bronchiolar diameter was determined for each dog at 26 days after inoculation from photographic prints with a digitizing tablet interfaced with a microcomputer and morphometric software (Bioquant II, R and M Biometrics, Nashville, TN).

Virology, Viral Serology, and Bacteriology

At necropsy samples of the caudal portion of the left cranial lung lobe were frozen in liquid nitrogen and stored at −65 C until viral isolation and titration were attempted. The lung samples from dogs at 2, 3, 5, 8, 15, and 26 days after inoculation were thawed, diluted 1:10 (weight/volume) in PBSS, and homogenized with Ten Broeck grinders at 4 C. The homogenates were clarified by centrifugation, and the supernatants were serially diluted and inoculated into wells of 96-well microtiter plates containing confluent monolayers of MDCK cells. The cells were maintained in Eagle's minimum essential medium supplemented with 10% fetal bovine serum and 1% of a penicillin, streptomycin, and antimycotic mixture (Gibco Laboratories, Grand Island, NY). Wells were examined for cytopathic effects at 7 days after inoculation of the wells, and viral titers ($TCID_{50}$) were calculated by the method of Reed and Muench.[28] Serum samples were collected at the start of the experiment and at necropsy from all dogs. Serum neutralizing antibody titers were determined by a modification of the method of Appel.[29] Samples of the left caudal lung lobe were cultured by routine techniques for bacterial pathogens.

Immunoperoxidase Antigen Localization

At necropsy the cranial portion of the left cranial lung lobe was perfused with 4% gelatin at 37 C as described[30] for maintaining the lung in an expanded state. The lobes were cooled to 4 C in iced water and sectioned into blocks. Blocks were mounted on balsa wood backing and then frozen in Freon 22 that had been cooled to −160 C in liquid nitrogen. Trachea was also frozen in

a similar manner without gelatin infusion. The blocks were sectioned at 8 μ on a cryostat microtome, and sections were stored at −65 C until they were stained for viral antigen. An indirect immunoperoxidase method was used. The primary antibody was prepared by hyperimmunizing a rabbit with CAV-2. Rabbit serum was adsorbed on monolayers of MDCK cells to remove nonspecific antibodies. Peroxidase-labeled goat anti-rabbit IgG was used as the second reagent. Sections were treated with nonimmunized goat serum after the gelatin had been dissolved in warm saline and prior to primary antibody treatment to decrease nonspecific staining. The enzymatic reaction was developed with 3,3′-diaminobenzidine.[31] CAV-2-infected MDCK cells on coverslips and lung sections with detectable intranuclear viral inclusions were used as positive controls. Uninfected MDCK cells on coverslips and tissue from known viral-negative lung were used as negative controls. Other controls, including running incubation procedures with primary specific antiserum deleted and after adsorbing specific antibodies from primary antiserum with concentrated virus, indicated that positive staining was specific for viral antigen.

Results

Macroscopic, Clinical, and Bacteriologic Findings

Control dogs were clinically normal and had no gross lesions at necropsy. Infected dogs had mild, dry coughs at 2, 3, and 4 days after inoculation and moderately elevated rectal temperature (up to 40 C) at 4–6 days. The first gross lesions were observed in dogs at 2 days after inoculation. There were red, depressed foci, 0.5–1.5 mm in diameter, scattered throughout the lung lobes. Similar lesions were observed in 1 dog at 3 days after inoculation. The other dog at 3 days had larger red, depressed, firm areas confined largely to cranial and ventral areas of the lung. The most severely affected lobe was the right middle lung lobe. Similar mild gross lesions were observed at 4, 5, and 8 days after inoculation, except in 1 dog at 8 days after inoculation that had diffusely condensed cranial and middle lung lobes. One dog died at 15 days after inoculation, and its cranial and middle lung lobes were diffusely pneumonic. Moderate numbers of *Pseudomonas aeruginosa* were isolated from the lung. No bacteria were isolated from the lungs of any of the other dogs. The other dog necropsied at 15 days after inoculation had several red, depressed areas 1–3 cm in diameter scattered in the cranial and middle lung lobes. Dogs at 26 days after viral infection had light red depressed foci 0.4–1.2 cm in diameter on the ventral margins of the right middle and cranial lung lobes.

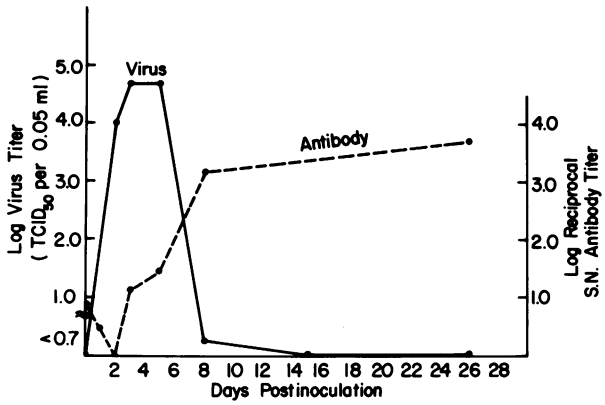

Figure 1—Viral titer (Log_{10}) in lung homogenates and serum neutralizing antibody titers (Log_{10}) in young dogs inoculated with canine adenovirus Type 2. Lung viral titers are expressed per 0.05 ml of 10% of lung homogenate.

Virology and Viral Serology

The results of the virologic and viral serologic studies are summarized in Figure 1. Virus was isolated from lung homogenates at 2, 3, 5, and 8 days after inoculation. Serum-neutralizing antibody was detected in serum before inoculation that represented passively acquired antibody from the vaccinated bitches. Antibody was first detected above preinoculation levels at 3 days after inoculation. The control dogs had no elevation from preinoculation levels throughout the course of the experiment.

Light and Electron Microscopy, Morphometry, and Immunoperoxidase

As early as 1 day after viral inoculation, intranuclear virions could be detected by transmission electron microscopy in nonciliated bronchiolar epithelial cells in terminal and respiratory bronchioles (Figure 2) as well as less frequently in mucous cells in bronchi and trachea. Immunoperoxidase staining for viral antigen demonstrated the presence of antigen most frequently in bronchiolar epithelial cells and less frequently in tracheal and bronchial epithelial cells. Viral antigen was also demonstrated in nuclei and cytoplasm of epithelial cells in the tracheal and bronchial submucosal glands (Figure 3). Viral particles were arranged in the nuclei of epithelial cells in crystalline arrays along with more finely granular material of low electron density (Figures 2 and 4). Viral assembly and release was associated with loss of the nuclear envelope and dispersion of assembled virions into the cytoplasm. Other cytopathologic changes in virus-infected nonciliated bronchiolar cells and mucous cells were swelling of endoplasmic reticulum and the nuclear envelope, swell-

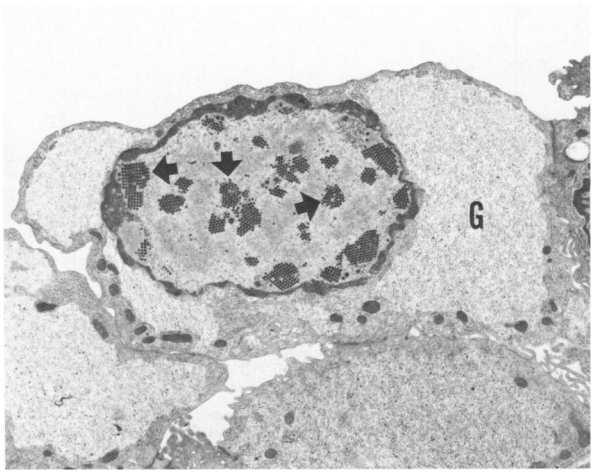

Figure 2—Respiratory bronchiole from a dog 1 day after viral inoculation. Crystalline arrays of assembled adenovirus (*arrows*) are present in the nucleus of an nonciliated bronchiolar epithelial cell. The cytoplasm contains abundant glycogen (*G*); which is a normal for nonciliated bronchiolar epithelial cells in dogs. (Transmission electron micrograph, ×4760)

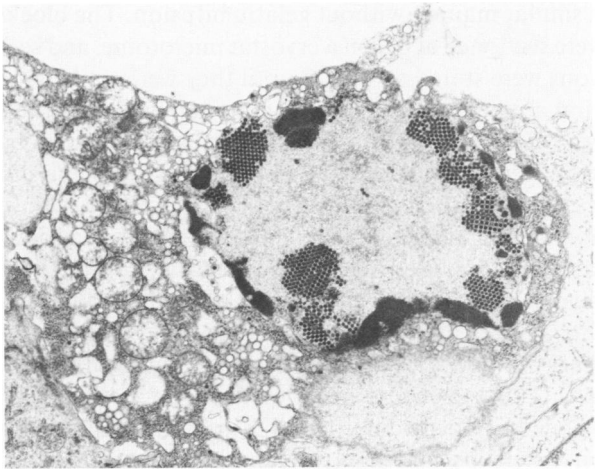

Figure 4—Nonciliated bronchiolar epithelial cell in the terminal bronchiole of a dog 2 days after adenoviral inoculation. Arrays of virions are in the nucleus, as well as finely granular material of low electron density. The nuclear envelope is ruptured. Endoplasmic reticulum and mitochondrial inner compartments in the cytoplasm are swollen. (Transmission electron micrograph, ×6300)

ing of mitochondrial inner compartments (Figure 4), and rupture of the plasmalemma.

At 2 days after viral inoculation, alterations in the bronchioles and small-caliber bronchi were characterized by hyperplasia of the bronchial and terminal and respiratory bronchiolar epithelium. Viral antigen distribution as determined by immunoperoxidase technique was comparable to that described for 1 day. The cell types contributing most to this multilayered, hypercellular epithelium in bronchioles and bronchi were nonciliated and devoid of secretory droplets. The cells often contained intranuclear viral inclusions in the most superficial layers (Figures 5 and 6). Macrophages and neutrophils were associated with these infected epithelial cells in the peribronchial and peribronchiolar connective tissue as well as between epithelial cells and in the airway lumen (Figures 5 and 6). In distal bronchi, there was mild hyperplasia of epithelial cells in submucosal glands and similar collections of neutrophils and macrophages in glandular lumens and in periglandular connective tissue. Ciliated epithelial cells were only minimally altered during the first days after viral inoculation. Virus particles could be found on the surface of ciliated bronchiolar epithelial cells and occasionally in membrane-bound vacuoles in cytoplasm. Virions in these cells were not observed in nuclei. Similar hyperplastic epithelial lesions in distal bronchi and

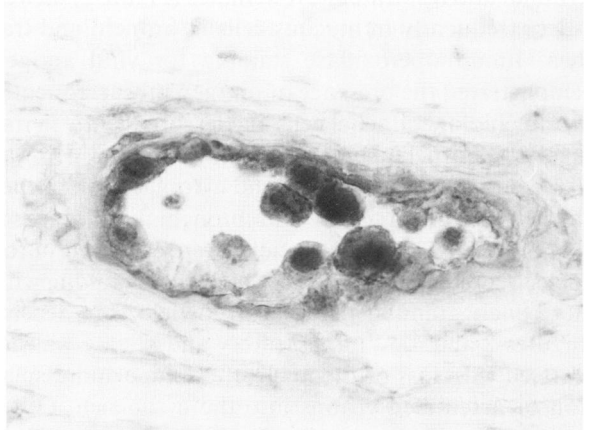

Figure 3—Submucosal gland from the bronchus of a dog 3 days after inoculation with adenovirus. Viral antigen in the nuclei and cytoplasm of glandular epithelial cells is positively stained. (Immunoperoxidase, ×498)

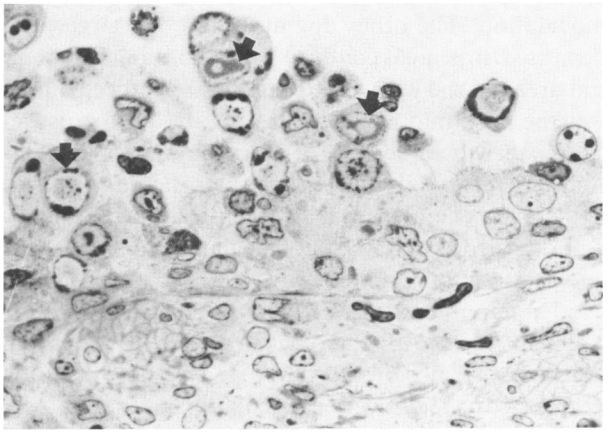

Figure 5—Terminal bronchiolar epithelium from a dog 2 days after inoculation with adenovirus. The epithelium is hypercellular and has multiple layers. Hypertrophied nonciliated epithelial cells with intranuclear inclusions (*arrows*) are present in the most superficial epithelial layers. Neutrophils and macrophages are in the lumen. (Epon-Araldite, toluidine blue, ×690)

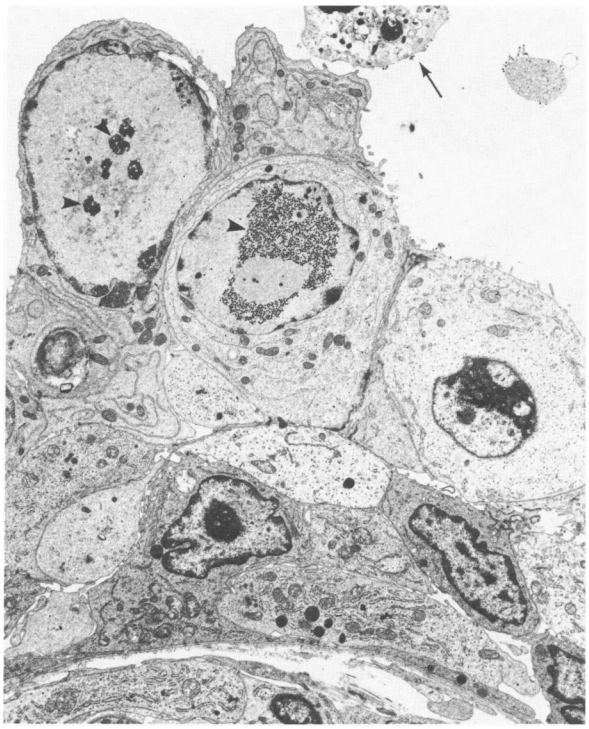

Figure 6—Terminal bronchiolar epithelium similar to that in Figure 5. The multilayered epithelial cells are hypertrophied nonciliated cells with intranuclear aggregates of adenovirus (*arrowheads*). Part of a neutrophil (*arrow*) is present in the upper portion of the field. (Transmission electron micrograph, ×2945)

terminal bronchioles were observed in infected dogs at 3 and 4 days after inoculation, but there was a more extensive inflammatory cell infiltration that also extended into alveolar parenchyma. Bronchial and bronchiolar walls were thickened and edematous and contained aggregates of neutrophils, macrophages, and lymphocytes. In dorsal and caudal lung areas, and to a lesser extent in cranial and ventral areas, inflammatory reactions were confined largely to bronchi, bronchioles, and a minimal amount of peribronchiolar alveolar parenchyma (Figure 7). In ventral regions of the lung, there were more extensive areas of inflammatory cell infiltration in alveolar parenchyma throughout lobules (Figure 8). Neutrophils, macrophages, and fibrin were present in alveoli. Viral antigen could be detected in alveolar epithelial cells and alveolar macrophages by immunoperoxidase technique. Viral particles were identified by transmission electron microscopy in nuclei and cytoplasm of Type 2 alveolar epithelial cells and also occasionally in low cuboidal and flattened alveolar epithelial cells with characteristics intermediate between Type 2 and Type 1 alveolar epithelial cells. Cytopathologic changes in nuclear envelopes, endoplasmic reticulum, and mitochondria similar to those observed in bronchiolar epithelial cells were found in alveolar epithelial cells that contained intranuclear viral aggregates. Virus was often observed in phagocytic vacuoles in alveolar macophages and neutrophils within alveolar spaces. Macrophages and neutrophils were present within interalveolar septa.

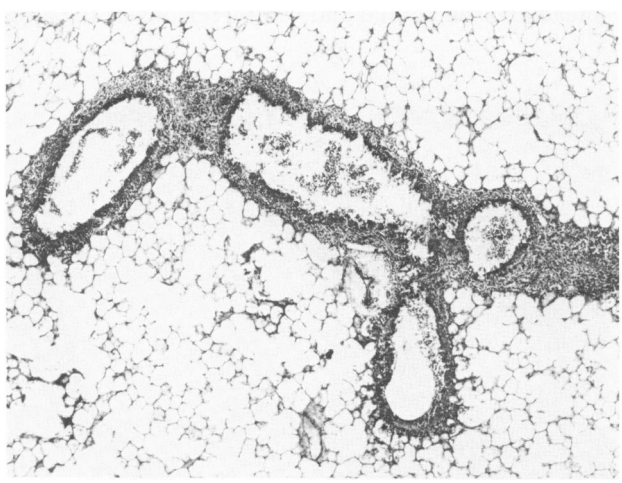

Figure 7—Terminal and respiratory bronchioles and surrounding alveolar parenchyma from a dog 3 days after viral inoculation. The bronchiolar lumens contain inflammatory cell exudate. The bronchiolar walls are thickened and infiltrated by inflammatory cells. Surrounding alveolar parenchyma is relatively free of inflammatory exudate. (Paraffin section, H&E, ×35)

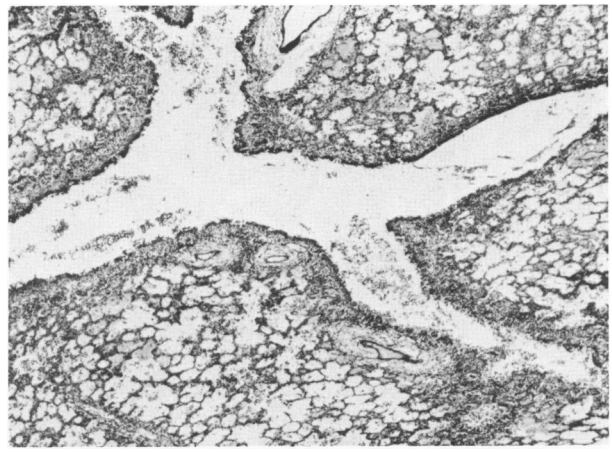

Figure 8—Respiratory bronchioles and surrounding alveolar parenchyma from the ventral portion of the right middle lobe of a dog 3 days after inoculation. The bronchiolar walls and surrounding interalveolar septa are thickened and hypercellular. Alveolar spaces contain cells and eosinophilic exudate. (Paraffin section, H&E, ×35)

At 5 and 8 days after inoculation, epithelium lining terminal and respiratory bronchioles was often completely eroded, and bronchiolar lumens contained necrotic cell debris, fibrin, and macrophages and neutrophils. In areas where epithelium remained, ciliated cells often had ultrastructural abnormalities, including loss of cilia and incorporation of basal bodies and axonemes into the cytoplasm (Figure 9), in addition to intracytoplasmic invaginations of the plasmalemma

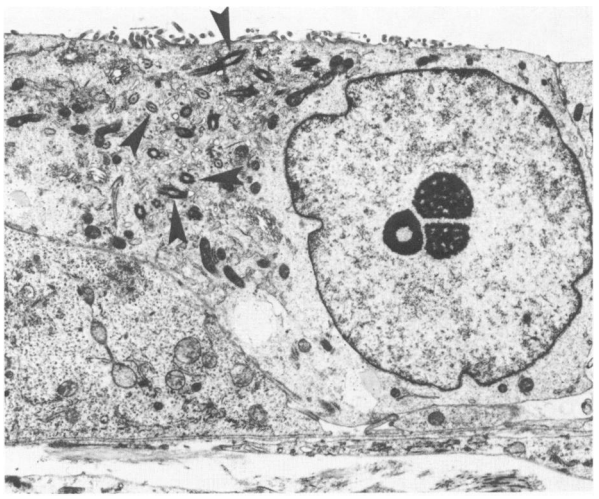

Figure 9—Ciliated cell from a terminal bronchiole of a dog 5 days after viral inoculation. The nucleus contains prominent nucleoli. Basal bodies and axonemes (*arrowheads*) are incorporated in the cytoplasm. The cell has no cilia projecting from its surface. (Transmission electron micrograph, ×4760)

that included cilia. There were dense aggregates of macrophages, lymphocytes, and neutrophils around and within bronchial glands and around bronchioles. There were occasional necrotic epithelial cells associated with these inflammatory cell aggregates. Increased numbers of loosely arranged fibroblasts were present in the submucosa of partially eroded bronchioles. In areas of pneumonia, there were increased numbers of Type 2 epithelial cells, and some alveoli were completely lined by these cells. Intranuclear viral inclusions and viral antigen were present in Type 2 cells in histologic and immunoperoxidase sections (Figure 10). There were collections of macrophages, lymphocytes, plasma cells, and occasional neutrophils in alveolar spaces and interalveolar septa. Small amounts of fibrin were also present in alveolar spaces.

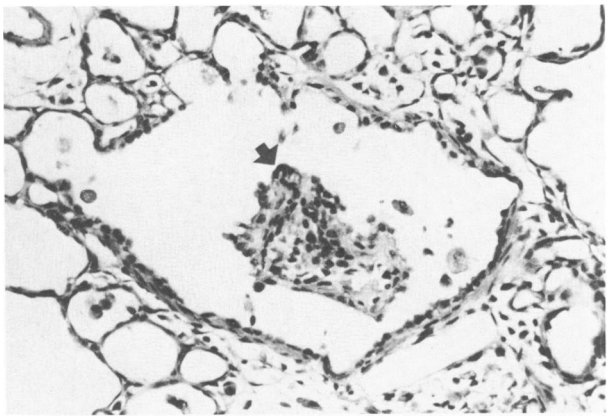

Figure 11—Respiratory bronchiole from a dog 15 days after viral infection. A polyp (*arrow*) of connective tissue containing mononuclear inflammatory cells protrudes into the bronchiolar lumen. (Paraffin section, H&E, ×72)

At 15 days after inoculation, terminal and respiratory bronchioles often had small areas of epithelial erosion. Viral inclusions and viral antigen were not present in tissue sections. In 1 of the 2 dogs examined at this time, fibrin, macrophages, and cell debris were present in many bronchiolar lumens and surrounding alveoli. Small polyps composed of collagen, fibroblasts, and inflammatory cells covered by low cuboidal epithelial cells were present in many terminal and respiratory bronchioles (Figure 11). Small collections of lymphocytes, plasma cells, and macrophages were present in the bronchiolar submucosa and peribronchiolar connective tissue and in surrounding interalveolar septa. In the other dog that died at this time, there were widespread areas in cranial and ventral regions of the lung

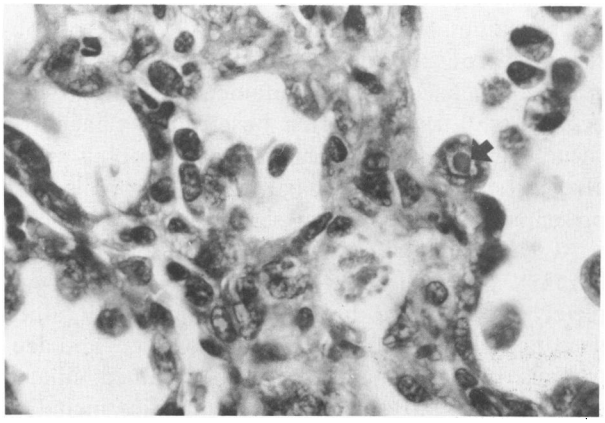

Figure 10—Alveolar parenchyma from a dog 8 days after viral inoculation. Alveolar septa are lined by cuboidal (Type 2) epithelial cells. One cell contains a prominent intranuclear viral inclusion (*arrow*). (Paraffin section, H&E, ×725)

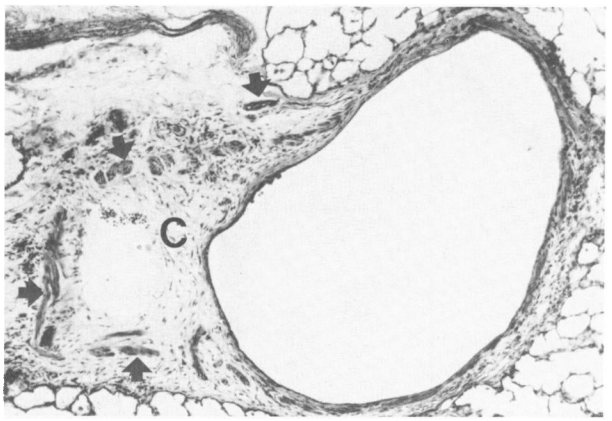

Figure 12—Terminal bronchiole from a dog 26 days after viral inoculation. The bronchiolar lumen is partially obstructed by connective tissue (*C*). Smooth-muscle bundles (*arrows*) indicate the former bronchiolar perimeter. (Paraffin section, H&E, ×72)

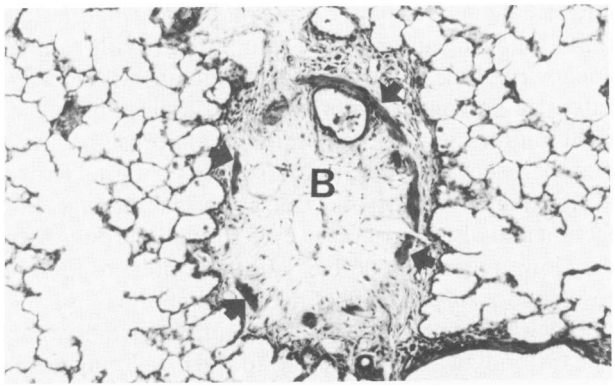

Figure 13—Terminal bronchiole from a dog 26 days after viral inoculation. The bronchiolar lumen (*B*) is almost completely replaced by connective tissue. Smooth muscle (*arrows*) outlines the former perimeter. (Paraffin section, H&E, ×72)

Table 1—Morphometric Data for Dogs at 26 Days After Infection

	Control dogs (n = 3)	Infected dogs (n = 3)
Body weight (kg)	4.30 ± 0.52*	3.68 ± 0.67
Left lung volume (cu cm)	145.80 ± 16.11	156.07 ± 13.36
Specific left lung volume (cu cm/100 g)	3.40 ± 0.37	4.29 ± 0.43†
Mean Terminal Bronchiole Area, Right lung (sq mm)	0.19 ± 0.06	0.12 ± 0.05
Mean terminal bronchiole area, right middle lobe (sq mm)	0.18 ± 0.04	0.09 ± 0.01‡

* Mean ± standard deviation.
† $P < 0.06$, two-sided t test.
‡ $P < 0.02$.

that contained dense aggregates of neutrophils, fibrin, and necrotic cell debris in bronchioles and throughout the surrounding alveolar parenchyma.

At 26 days after inoculation, there was partial or complete stenosis of many terminal bronchioles by tissue composed of fibroblasts, small numbers of lymphocytes and macrophages, and collagen (Figures 12–14). In many instances there was distortion and fibrosis of surrounding alveolar parenchyma (Figure 13). These areas of bronchiolar obliteration or stenosis and parenchymal fibrosis were present most frequently in ventral areas of the lung and were found in all 3 dogs that had been infected. Bronchiolar narrowing was associated with a significant reduction in mean terminal bronchiolar cross-sectional area only in the right middle lobe (Table 1). There was no significant reduction in overall terminal bronchiolar cross-sectional area for the entire right lung. The lung volumes of infected dogs, although higher than controls, were not significantly different. In bronchioles partially narrowed by collagenous connective tissue, the epithelial lining was often composed of squamous or nonciliated cuboidal cells that were sometimes arranged in multiple layers, in contrast to ciliated and nonciliated bronchiolar cells that were observed in controls (Figures 15 and 16). There was also increased density of collagen and small aggregates of macrophages, lymphocytes, and plasma cells in the submucosa of small caliber bronchi and around bronchial glands.

Discussion

The results of this study demonstrate that bronchiolitis obliterans can be induced in young dogs by ex-

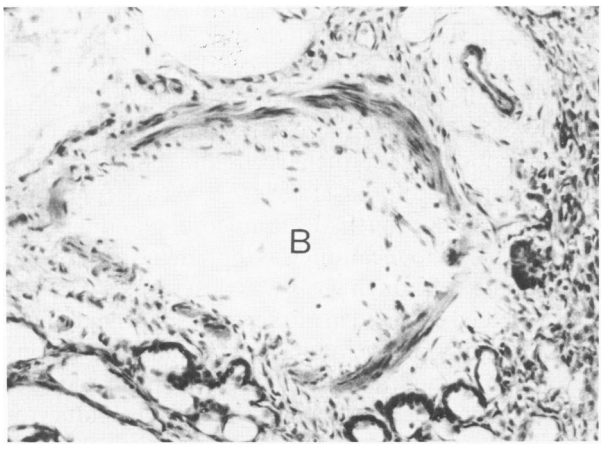

Figure 14—Terminal bronchiole and surrounding parenchyma from a dog 26 days after viral inoculation. The bronchiolar lumen (*B*) is replaced by connective tissue, and surrounding interalveolar septa are distorted and thickened by collagenous connective tissue. (Paraffin section, H&E, ×170)

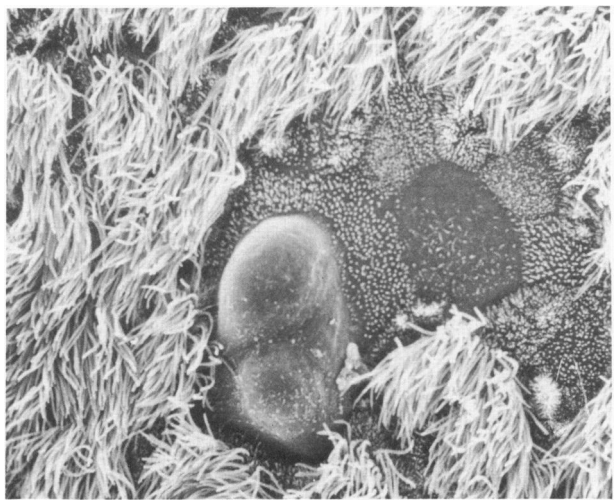

Figure 15—Terminal bronchiolar epithelium from a control dog 26 days after sham inoculation. Ciliated and nonciliated epithelial cells are present. (Scanning electron micrograph, ×2400)

Figure 16—Epithelium lining a partially stenotic terminal bronchiole from a dog 26 days after inoculation. The epithelial lining is nonciliated. (Scanning electron micrograph, ×3000)

perimental adenovirus infection. Adenoviral infection is an occasional cause of clinical bronchiolitis and pneumonia in children[5,10] that can result infrequently in serious clinical disease.[4,11-16] The pathologic changes described in children with serious clinical disease resulting from adenovirus infection include necrotizing bronchitis and bronchiolitis with necrosis of bronchial glandular epithelium, bronchiectasis, bronchiolitis obliterans, interstitial pneumonia, and pulmonary fibrosis.[4,11-16] Adenoviral pulmonary disease is also a problem among immunocompromised individuals.[32]

Experimental animal models of adenoviral bronchiolitis and pneumonia have been previously described,[22-24] but their usefulness for experimental pathogenesis studies and studies on therapeutic or preventive modulators of disease has not been determined. Natural adenoviral respiratory disease is recognized in a wide range of animals.[33] Although a recently described model using cotton rats and human adenovirus may be useful for immunologic and virologic studies, only very mild lesions are induced,[24] and the model may be only of limited use for studies focused on structural and functional alterations induced by infection. Models using nonhuman primates have also been described,[23,34] but the scarcity and cost of these animals may be prohibitive to extensive experimental studies.

The experimental model described in this report uses the dog and a natural adenoviral pathogen of that species. The lesions that are induced experimentally are comparable in distribution and severity to those described in children manifesting serious adenoviral respiratory disease.[12,16] Necrotizing bronchitis and bronchiolitis with necrosis of bronchial glands as well as interstitial pneumonia are acute pathologic manifestations following infection of young dogs with canine adenovirus Type 2. Bronchiolitis obliterans with locally extensive narrowing of bronchioles, especially in the right middle lung lobe, and multifocal fibrosis of alveolar parenchyma are chronic sequelae of the virus-initiated inflammatory reaction and tissue damage. Infection and disease occurred even though the dogs had very low, maternally derived antibody titers to the virus. It is not surprising that the low level of passive antibody was not protective; however, the possibility that the antibody was contributing to the development of pulmonary lesions needs to be considered.[1] The uneven distribution of severe lesions could, at least in part, be the result of intratracheal viral inoculation that would be expected to lead to inhomogeneous distribution of virus.

Bronchiectasis was not a change in the dogs 26 days after infection. It may be that the bronchiectasis following adenoviral infection requires secondary bacterial infection or a more prolonged viral replicative period than occurred in this experimental system. Bronchiectasis has also been suggested to be a long-term sequelae of adenovirus-induced necrotizing bronchitis and bronchiolitis obliterans following stagnation of secretions and stimulation of chronic inflammation.[16] Pulmonary hyperinflation has been described in adenoviral infections in children.[4] Although there was an increase in specific lung volume in the infected dogs at 26 days after infection, the increase was not statistically significant. It has been demonstrated that rats infected with parainfluenza virus during periods of postnatal lung growth have transiently higher absolute and specific lung volumes than control rats, possibly due to a transient stimulation of lung growth following infection.[21]

The severe necrotizing and hyperplastic bronchitis and bronchiolitis in this canine model was associated with adenoviral replication in nonciliated bronchiolar epithelial cells and mucous cells. The hyperplastic epithelial lesions appeared to be due to increases in nonciliated bronchiolar epithelial cells and, possibly, postmitotic mucous and basal cells.[35,36] Virus replication also occurred in bronchial submucosal glandular epithelium. Viral replication was not demonstrated in ciliated cells. Although virus was observed on the surface of ciliated cells and in intracytoplasmic membrane-bound vacuoles, no intranuclear assemblies of virions were demonstrated. The virus observed in ciliated cells may have been incorporated in the cells by endocytosis. Evidence of injury to ciliated cells in virus-infected dogs was observed. The loss of surface cilia and incorporation of basal bodies and axonemes into the

cytoplasm has been observed previously in ciliated cells during other respiratory viral infections.[21,37] This alteration in ciliated cells could be a manifestation of virus-induced cytotoxic effects associated with nonproductive infection or of injury mediated by inflammatory cells. It could also be a nonspecific manifestation following injury to adjacent nonciliated cells.

The pathogenesis of the bronchiolitis obliterans in this experimental infection remains to be more precisely delineated. Bronchiolitis obliterans occurs after viral induced epithelial necrosis and erosion with obstruction of the bronchiolar lumens by fibrin, necrotic debris, and inflammatory cells. The pathogenesis of the bronchiolitis obliterans after adenovirus infection has been discussed.[16] The epithelial necrosis and delayed epithelial repair with accumulation of exudate in small caliber airways could stimulate organization of the exudate by collagenous connective tissue. The specific roles that epithelial necrosis and organization of exudate play as opposed to active stimulation of fibrosis by mediators released from macrophages and other cells participating in the inflammatory and immunologic responses[38] in these virus-induced bronchiolar lesions require more detailed experimental examination.

The virus-initiated bronchiolar injury described in this study did result in persistent narrowing of bronchioles in locally extensive areas of the lung. Bronchiolar stenosis and complete obliteration of terminal bronchioles would be expected to result in increased airway resistance similar to that reported in children recovering from viral bronchiolitis during early life.[3,6,7,9] Furthermore, the failure of epithelial cells in damaged bronchioles to generate a normal density of ciliated cells could be associated with depressed mucociliary clearance in these airways.

The interstitial pneumonia resulting from this experimental infection in dogs was associated with adenoviral replication in Type 2 alveolar epithelial cells. Viral particles were observed in phagosomes of alveolar macrophages and in the nuclei of cells with intermediate characteristics between Type 2 and Type 1 alveolar epithelial cells. Although other investigators have described viral replication in Type 1 alveolar epithelial cells,[39,40] it seems more likely that the flattened cells observed containing virions were Type 2 cells that were spreading out across the damaged alveolar septal surface.

In summary, the results of this study demonstrate that experimental canine adenovirus Type 2 infection in dogs results in severe necrotizing bronchitis and bronchiolitis that is followed by bronchiolitis obliterans. This infection in dogs may serve as a useful experimental model of viral bronchiolitis in infants for studies designed to evaluate physiologic and structural alterations following viral infection in early life.

References

1. Wohl MEB, Chernick V: Bronchiolitis. Am Rev Resp Dis 1978, 118:759–781
2. Aherne W, Bird T, Court SDM, Gardner PS, McQuillin J: Pathologic changes in virus infections of the lower respiratory tract in children. J Clin Pathol 1970, 23:7–18
3. Wohl MB, Stigol LC, Mead J: Resistance of the total respiratory system in healthy infants and in infants with bronchiolitis. Pediatrics 1969, 43:495–509
4. Gold R, Wilt JC, Adhikari PK, Macpherson RI: Adenoviral pneumonia and its complications in infancy and childhood. J Can Assoc Radiol 1969, 20:218–224
5. Henderson FW, Clyde WA, Collier AM, Denny FW, Senior RJ, Sheaffer CI, Conley WG, Christian RM: The etiologic and epidemiologic spectrum of bronchiolitis in pediatric practice. J Pediatr 1979, 95:183–190
6. Sims DG, Downham MAPS, Gardner PS, Webb JKG, Weightman D: Study of 8-year-old children with a history of respiratory syncytial virus bronchiolitis in infancy. Br Med J 1978, 1:11–14
7. Kattan M, Keens TG, Lapierre JG, Levison H, Bryan AC, Reilly BJ: Pulmonary function abnormalities in symptom-free children after bronchiolitis. Pediatrics 1977, 59:683–688
8. Colley JRT, Douglas JWB, Reid DD: Respiratory disease in young adults: Influence of early childhood lower respiratory tract illness, social class, air pollution, and smoking. Br Med J 1973, 3:195–198
9. Simila S, Linna O, Lanning P, Heikkinen E, Ala-Houhala M: Chronic lung damage caused by adenovirus type 7: A ten-year follow-up study. Chest 1981, 80:127–131
10. Gardner PS: How etiologic, pathologic, and clinical diagnoses can be made in a correlated fashion. Pediatr Res 1977, 11:254–261
11. Chany C, Lepine P, Lelong M, Le-Tan-Vinh, Satge P, Virat J: Severe and fatal pneumonia in infants and young children associated with adenovirus infections. Am J Hyg 1958, 67:367–378
12. Becroft DMO: Histopathology of fatal adenovirus infection of the respiratory tract of young children. J Clin Pathol 1967, 20:561–569
13. Lang WR, Howden CW, Laws J, Burton JF: Bronchopneumonia with serious sequelae in children with evidence of adenovirus type 21 infection. Br Med J 1969, 1:73–79
14. Simila S, Ylikorkala O, Wasz-Hockert O: Type 7 adenovirus pneumonia. J Pediatr 1971, 79:605–611
15. James AG, Lang WR, Liang AY, Mackay RJ, Morris MC, Newman JN, Osborne DR, White PR: Adenovirus type 21 bronchopneumonia in infants and young children. J Pediatr 1979, 95:530–533
16. Becroft DMO: Bronchiolitis obliterans, bronchiectasis, and other sequelae of adenovirus type 21 infection in young children. J Clin Pathol 1971, 24:72–82
17. Collier AM, Clyde WA: Model systems for studying the pathogenesis of infections causing bronchiolitis in man. Pediatr Res 1977, 11:243–246
18. Prince GA, Jenson AB, Horswood RL, Camargo E, Chanock RM: The pathogenesis of respiratory syncytial virus infection in cotton rats. Am J Pathol 1978, 93:771–792
19. Taylor G, Stott EJ, Hughes M, Collins AP: Respiratory syncytial virus infection in mice. Infect Immun 1984, 43:649–655
20. Wagener JS, Minnich L, Sobonya R, Taussig LM, Ray CG, Fulginiti V: Parainfluenza type II infection in dogs:

A model for viral lower respiratory tract infections in humans. Am Rev Resp Dis 1983, 127:771–775
21. Castleman WL: Alterations in pulmonary ultrastructure and morphometric parameters induced by parainfluenza (Sendai) virus in rats during postnatal growth. Am J Pathol 1984, 114:322–335
22. Swango LJ, Wooding WL, Binn LN: A comparison of the pathogenesis and antigenicity of infectious canine hepatitis virus and the A26/61 virus strain (Toronto). Am J Vet Res 1970, 156:1687–1696
23. Boyce JT, Giddens WE, Valerio M: Simian adenoviral pneumonia. Am J Pathol 1978, 91:259–276
24. Pacini DL, Dubovi EJ, Clyde WA: A new animal model for human adenoviral respiratory disease. J Inf Dis 1984, 150:92–97
25. Appel M, Bistner SI, Menegus M, Albert DA, Carmichael LE: Pathogenicity of low-virulence strains of two canine adenovirus types. Am J Vet Res 1973, 34:543–550
26. Castleman WL, Dungworth DL, Schwartz LW, Tyler WS: Acute respiratory bronchiolitis: An ultrastructural and autoradiographic study of epithelial injury and renewal in rhesus monkeys exposed to ozone. Am J Pathol 1980, 98:811–840
27. Scherle W: A simple method for volumetry of organs in quantitative stereology. Mikroskopie 1970, 26:57–60
28. Hawkes RA: General principles underlying laboratory diagnosis of viral infections, Diagnostic Procedures for Viral, Rickettsial and Chlamydial Infections. 5th edition. Edited by EH Lennette, NJ Schmidt. Washington, DC, American Public Health Association, 1979, pp 34–35
29. Appel M, Robson DS: Microneutralization test for canine distemper virus. Am J Vet Res 1973, 34:1459–1463
30. Castleman WL, Dungworth DL, Tyler WS: Cytochemically detected alterations of lung acid phosphatase reactivity following ozone exposure. Lab Invest 1973, 29:310–319
31. Sternberger LA: Immunocytochemistry. 2nd edition. New York, John Wiley and Sons, 1979, pp 96–99, 124–127
32. Zahradnik JM, Spencer MJ, Porter DD: Adenovirus infection in the immunocompromised patient. Am J Med 1980, 68:725–732
33. Gillespie JH, Timoney JF: The Adenoviridae, Hagan and Bruner's Infectious Diseases of Domestic Animals. 7th edition. Ithaca, Cornell University Press, 1981, pp 506–520
34. Moe JB, Osburn BI, Schwartz LW, Anderson J, Johnson KP: Experimental adenovirus SV-20 pneumonia in fetal rhesus monkeys: Pathologic and virologic studies. Lab Invest 1979, 41:211–219
35. Kauffman SL: Cell proliferation in the mammalian lung. Int Rev Exp Pathol 1980, 22:131–191
36. Keenan KP, Combs JW, McDowell EM: Regeneration of hamster tracheal epithelium after mechanical injury: II. Multifocal lesions: Stathmokinetic and autoradiographic studies of cell proliferation. Virchows Arch [Cell Pathol] 1982, 41:215–229
37. Castleman WL, Chandler SK, Slauson DO: Experimental bovine respiratory syncytial virus infection in conventional calves: Ultrastructural respiratory lesions. Am J Vet Res 1985, 46:554–560
38. Rennard SI, Bitterman PB, Crystal RG: Pathogenesis of granulomatous lung diseases: IV. Mechanisms of fibrosis. Am Rev Resp Dis 1984, 130:492–496
39. Langloss JM, Hoover EA, Kahn DE: Diffuse alveolar damage in cats induced by nitrogen dioxide or feline calicivirus. Am J Pathol 1977, 89:637–648
40. Ward JM, Houchen DP, Collins MJ, Young DM, Reagan RL: Naturally-occurring Sendai virus infection in athymic nude mice. Vet Pathol 1976, 13:36–46

Acknowledgments

The author appreciates the generous and helpful advice of Dr. Max Appel and the technical assistance of Emery Schiff.